



Determination of dose-response calibration curves for gamma radiation using gamma-H2AX immunofluorescence based biodosimetry

Solomon Raj Jose¹, Peace Balasingh Timothy², Suganthy J³, Selvamani Backianathan², Soosai Manickam Amirtham⁴, Sandya Rani⁵, Rabi Singh²

¹Department of Radiotherapy, Christian Medical College Vellore, Vellore, India

²Department of Radiation Oncology, Christian Medical College Vellore, Vellore, India

³Department of Anatomy, Christian Medical College Vellore, CMC, Bagayam, Vellore, India

⁶Department of Physiology, Christian Medical College and Hospital Vellore, Vellore, India

⁵Centre for Stem Cell Research, Christian Medical College, Vellore, India

ABSTRACT

Background: Gamma-H2AX immunofluorescence assay has gained popularity as a DNA double strand break marker. In this work, we have investigated the potential use of gamma H2AX immunofluorescence assay as a biological dosimeter for estimation of dose in our institution.

Materials and methods: Seven healthy individuals were selected for the study and the blood samples collected from the first five individuals were irradiated to low doses (0–10 cGy) and high doses (50–500 cGy) in a telecobalt unit. All the samples were processed for gamma-H2AX immunofluorescence assay and the dose-response calibration curves for low and high doses were determined. In order to validate the determined dose-response calibration curves, the blood samples obtained from the sixth and seventh subjects were delivered a test dose of 7.5 cGy and 250 cGy. In addition, time and cost required to complete the assay were also reported.

Results: The goodness of fit (R^2) values was found to be 0.9829 and 0.9766 for low and high dose-response calibration curves. The time required to perform the gamma-H2AX immunofluorescence assay was found to be 7 hours and 30 minutes and the estimated cost per sample was 5000 rupees (~ 60 USD).

Conclusion: Based on this study we conclude that the individual dose-response calibration curves determined with gamma-H2AX immunofluorescence assay for both low and high dose ranges of gamma radiation can be used for biological dosimetry. Further, the gamma-H2AX immunofluorescence assay can be used as a rapid cost-effective biodosimetric tool for institutions with an existing confocal microscope facility.

Key words: radiation biology; molecular biology; radiation oncology

Rep Pract Oncol Radiother 2024;29(2):164–175

Address for correspondence: Solomon Raj Jose, Christian Medical College Vellore, Radiotherapy, Vellore, India; e-mail: josesarc@gmail.com

This article is available in open access under Creative Common Attribution-Non-Commercial-No Derivatives 4.0 International (CC BY-NC-ND 4.0) license, allowing to download articles and share them with others as long as they credit the authors and the publisher, but without permission to change them in any way or use them commercially

Introduction

Biodosimetry is the primary method of radiation dose assessment for nuclear excursion events, radiation accidents or occupational over-exposure events [1, 2]. The investigation of radiation exposure above 0.5 Gy is of utmost importance due to the manifestation of deterministic effects and onset of acute radiation syndrome in the event of whole-body exposure [3]. In addition, to assess the probability of late stochastic effects, the measurement of low doses below 10 cGy is considered vital [4]. Though the current gold standard method for biological dosimetry is dicentric chromosome assay (DCA), dose estimation with DCA is time consuming (3–4 days) and the minimal resolvable dose is limited to 10 cGy [5, 6]. These limitations call for the development of an alternative biological dosimeter that would play a vital role in the assessment of radiation dose in the absence of physical dosimetry and one that will be viable for the rapid dose estimation of both low and high dose ranges of ionizing radiation [7, 8].

In recent years, gamma-H2AX assay has been developed as a rapid biomarker to detect the DNA damage for low doses below 10 cGy as well as higher doses greater than 10 cGy [9, 10]. When ionizing radiation induces DNA double strand breaks (DSBs) in mammalian cells, various global response, such as cell death, cell repair and mis-repair which can occur in the cellular level [11]. One of the markers for signaling DSBs within the cell is the phosphorylation of the gamma-H2AX, a variant of the H2A protein that is found in the histone core of the DNA [12–14]. The gamma-H2AX can be quantified as foci by raising an anti-gamma-H2AX primary antibody followed by fluorescent-labelled secondary antibody which can be visualized under a fluorescence microscope [15, 16]. In this work, we have focused on the determination of dose-response calibration curves for both low dose and high dose ranges of gamma radiation using immunofluorescence-based gamma H2AX assay and the validation of the same. In addition, the essential steps for standardization as well as time and cost requirement for establishing the gamma-H2AX by immunofluorescence method as a biological dosimeter have been investigated and reported.

Materials and methods

Sample collection

Blood samples of 15 mL were collected from seven healthy individuals (4 male and 3 female), with ages ranging between 24–35 years, under sterile conditions. Consent was obtained prior to the blood sample collection and the research work was approved by institutional ethics committee.

Sample segregation

For the determination of dose response curves, blood samples obtained from first five individuals were exposed to known radiation doses of 0, 1, 5, and 10 cGy for low dose response assessment and 50, 100, 200, 300, and 500 cGy for high dose response assessment. For the purpose of test dose validation, samples obtained from the sixth and seventh individual were exposed to 7.5 cGy and 250 cGy such that they fell in the low and high dose range, respectively.

Set-up for irradiation

For the determination of dose-response calibration curves, the blood samples were exposed to gamma radiation in Theratron Equinox™ 80 telecobalt unit (TeamBest®, Ontario, Canada) which contains Cobalt-60 radioactive source (average energy — 1.25 MeV). For determination of low dose response calibration curves, samples were irradiated to doses of 0, 1, 5, and 10 cGy, and for high dose response calibration curves the samples were irradiated to doses of 50, 100, 200, 300 and 500 cGy, respectively. The temperature during the time of irradiation was maintained at 37°C using a temperature-controlled water phantom in order to simulate the human body temperature and to allow repair during irradiation (Fig. 1). The source to surface distance (SSD) was kept at 80 cm for a field size of 20 x 20 cm² at a dose-rate of 1.07 Gy/min. The set-up for irradiation is shown in Figure 1. For test dose validation, the samples obtained from the sixth and seventh individuals were exposed to test doses of 7.5 cGy and 250 cGy, respectively.

Physical dosimetry considerations

As mandated by international atomic energy agency (IAEA), prior to determination of calibration curves for biodosimetric studies, dose verification using physical dosimetry was performed using a 0.6 cm³

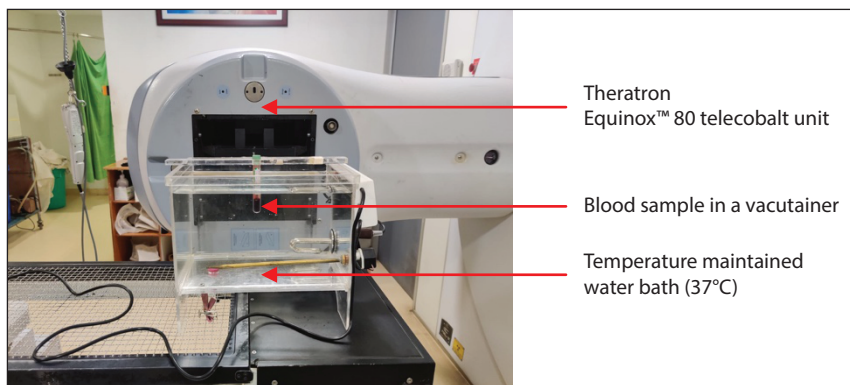


Figure 1. Setup for blood sample irradiation in Theratron Equinox 80C

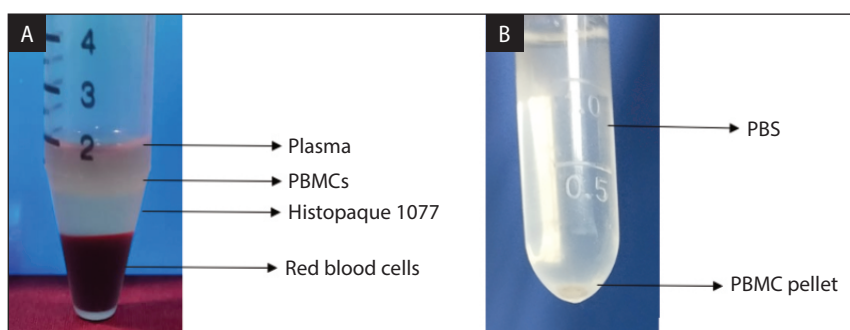


Figure 2. Segregation of peripheral blood mononuclear cells (PBMCs) after irradiation. **A.** Appearance of buffy coat consisting of PBMCs after gradient centrifuge method; **B.** PBMC pellet formation after the phosphate-buffered saline (PBS) wash

farmer-type ionization chamber and water-equivalent slab phantoms (Physikalisch-Technische Werkstätten (PTW), Germany) [2].

Sample preparation

Initially, the peripheral blood mononuclear cells (PBMCs) from the whole blood samples were isolated using gradient centrifuge method for which the whole-blood sample was gently added over Histopaque 1077 (Sigma) in a 1:1 ratio and centrifuged at 1500 rpm for 30 minutes. The buffy coat containing the PBMCs which appear between the Histopaque 1077 and the plasma was aspirated as shown in Figure 2A. Later, the PBMCs were washed thrice using phosphate-buffered saline (PBS) and stored in micro vials as shown in Figure 2B.

Protocol for immunofluorescent staining of gamma-H2AX assay

The gamma-H2AX protocol followed in this study was performed as per Chaurasia et al.

and Redon et al. with slight modifications [17, 18]. The 45-minute time interval between irradiation and processing of the whole blood in our experiment was kept consistent throughout the entire process. This time frame was considered an important factor as the gamma-H2AX expression increases after 30 min after irradiation and reaches its peak at 2 hours followed by a decay process due to repair of DNA DSBs [19]. To activate histone phosphorylation, the PBMCs were treated with fetal bovine serum and incubated for 30 minutes. The cell fixation was carried out by adding the PBMCs with 2% paraformaldehyde for 15 minutes and washed with PBS. Later, the cells were treated with 70% ethanol pre-cooled to minus 20°C for 20 minutes and washed with PBS. After wash, the cells were treated for antigen retrieval and protein blocking with PBS, 0.5% of Tween 20 and 0.1% of Triton X 100 (PBSTT) and 5% bovine serum albumin (BSA), for 30 minutes. The cells were first incubated for 2 hours using the primary antibody [Rabbit monoclonal anti gamma-H2AX antibody (1:500 di-

lution)] that was added to the cells with PBSTT and 1% BSA at room temperature. These cells were once again incubated with secondary antibody IgG (H+L) Highly Cross-Adsorbed Goat anti-Rabbit IgG, Alexa Fluor® 488 (A11034,1:200 dilution in 1% BSA with PBSTT) for one hour at room temperature followed by nuclear staining by addition of 4',6-diamidino-2-phenylindole (DAPI). An attempt to compare the effect of reducing the incubation time of primary and secondary antibody was also carried out.

Slide preparation

The cells were overlaid on to the microscopic slide by performing cytopspin at 500 rpm for 5 minutes and were mounted with 90% glycerol and a coverslip was placed over it. To immobilize the coverslip, the corners were sealed with nail polish. A comparison of gamma-H2AX foci analysis with and without cytopspin procedure was also performed.

Imaging and gamma-H2AX foci evaluation

Images were captured after the slide preparation using the Olympus laser scanning confocal microscope system (spectral version), Olympus FV1000 with 100 X magnification. The laser lines used were 405 nm for DAPI and multi argon laser line 488 nm for gamma-H2AX for fluorescence imaging. The gamma-H2AX foci were counted using “find maxima” plugin available in Fiji software [20]. For each dose point, 100 gamma-H2AX foci per cell were analyzed.

Time and cost requirement for gamma-H2AX immunofluorescence assay

To estimate the total time required to perform the assay, we noted the time required to perform each step while performing gamma H2AX immunofluorescence assay. The cost required to establish the same was also investigated and noted.

Statistical analysis

The statistical analysis was carried out using the Statistical Package for Social Sciences (SPSS) software Version 21.0 (Armonk, NY: IBM Corp). For the continuous data, descriptive statistics, such as mean \pm SD, was calculated. The R^2 statistics (goodness of fit) for the dose-response curves were also computed.

Results

Determination of dose response calibration curves

The gamma-H2AX immunofluorescence assay of the irradiated blood samples for five individuals was carried out and the corresponding foci per cell image for one of the subjects is depicted in Figure 3. It was observed that as the dose increased, the gamma-H2AX foci per cell also increased, representing the elevated levels of DNA DSBs. The mean low dose-response curve (low dose vs. gamma-H2AX foci per cell) from the irradiated blood samples of the five subjects showed a marked increase in foci per cell with increases in the low dose range (0–10 cGy). The goodness of fit was performed and the R^2 value was 0.9829, proving that there is a strong correlation between low dose and gamma-H2AX foci per cell as shown in Figure 4. The mean high dose-response curve (high dose vs. gamma-H2AX foci per cell) obtained from five subjects also showed a dose-dependent increase in gamma-H2AX foci per cell (50–500 cGy), and the R^2 value was 0.9766 as shown in Figure 5. The control cells (0 Gy), on average, consisted of 1.92 ± 0.49 gamma-H2AX foci per cell.

For each individual, the dose and gamma-H2AX foci per cell are represented in Table 1 and 2. The data show the mean of 100 cells analyzed (\pm standard deviation) per dose point, for each individual for the low dose (0–10 cGy) and high dose (50–500 cGy) range. Table 1 and 2 show a strong correlation between foci formation and doses (low and high) for all five subjects. From the mean low dose-response curve, the mathematical equation computed using linear fit model is as follows:

$$y = 0.3271x + 2.0916 \quad (1)$$

$$x = \frac{y - 2.0916}{0.3271} \quad (2)$$

where:

y is the mean gamma-H2AX foci per cell,

x is the dose (cGy),

a coefficient is 0.3271,

Intercept = 2.0916.

Similarly, from the mean dose response curve for the high dose range, the equation obtained using linear fit is as follows:

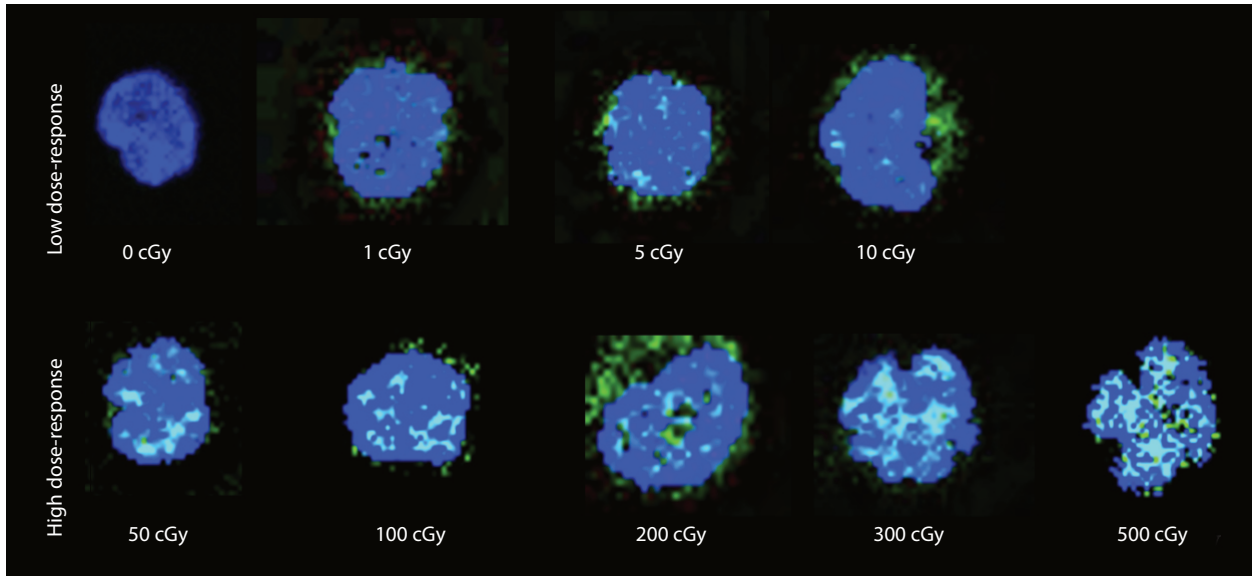


Figure 3. Radiation induced gamma-H2AX foci for low and high dose ionizing radiation. The green fluorescence (Alex fluor 488®) indicates the presence of gamma-H2AX at the site of DNA DSBs within the cell nuclei and the blue fluorescence (DAPI) represents the cell nuclei

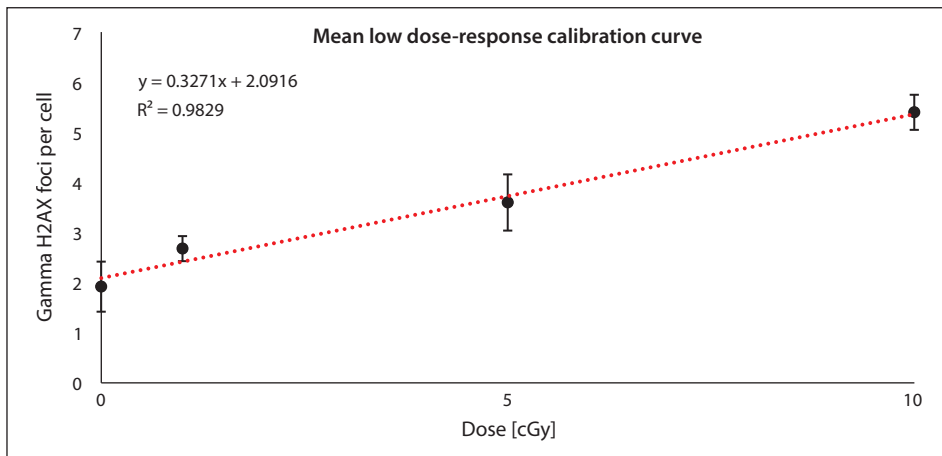


Figure 4. Mean gamma-H2AX foci per cell for low dose-response calibration curve of five individuals. [(100 cells per dose point) × 5 individuals = 500 cells in total per dose point] was plotted in this graph. The error bars represent standard deviation. Linear model was fit and the mathematical expression for the same was computed

$$y = 0.0267x + 6.0456 \quad (3)$$

$$x = \frac{y - 6.0456}{0.0267} \quad (4)$$

where:

y is the mean gamma-H2AX foci per cell,

x is the dose (cGy),

α coefficient is 0.0267,

Intercept = 6.0456.

Test dose validation of the determined dose response calibration curves

The validation results of the test dose in the low dose range was computed using the equation 2 and were found to be comparable to those of the administered dose with a dose difference of + 1.02 cGy and + 0.90 cGy for the blood samples obtained from subjects 6 and 7 as shown in Table 3. Similarly, for high dose, test dose validation was computed

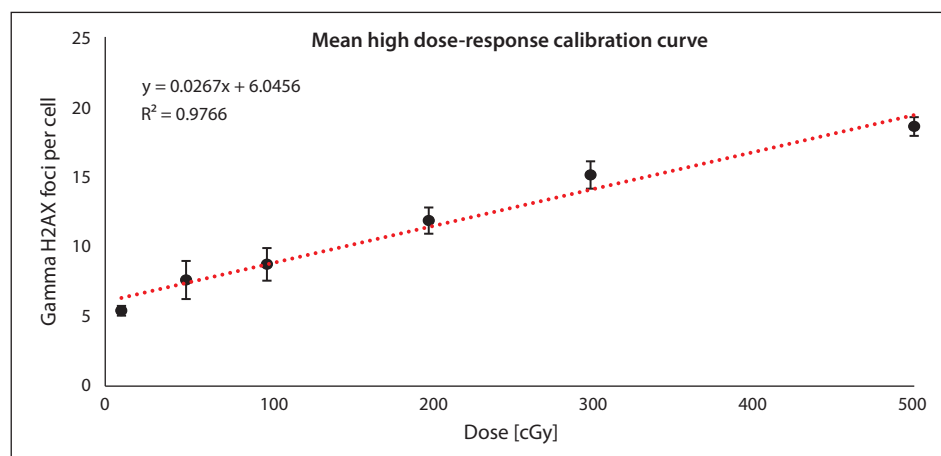


Figure 5. Mean gamma-H2AX foci per cell for high dose-response calibration curve of five individuals. [(100 cells per dose point) \times 5 individuals = 500 cells in total per dose point was plotted in this graph]. The error bars represent standard deviation. Linear model was fit and the mathematical expression for the same was computed

Table 1. Average values of gamma-H2AX foci per cell for low dose range

		Dose [cGy]			
Donors		0	1	5	10
Gamma-H2AX foci/per cell (average of 100 cells per dose point)	Individual 1	2.11 \pm 1.48	2.64 \pm 1.06	3.07 \pm 1.72	4.91 \pm 1.50
	Individual 2	1.56 \pm 1.17	3.08 \pm 1.51	4.48 \pm 1.75	5.53 \pm 1.77
	Individual 3	2.61 \pm 1.68	2.67 \pm 1.07	3.82 \pm 1.94	5.59 \pm 2.13
	Individual 4	1.33 \pm 1.14	2.38 \pm 1.71	3.3 \pm 1.73	5.18 \pm 1.93
	Individual 5	1.98 \pm 1.29	2.62 \pm 1.06	3.32 \pm 1.75	5.80 \pm 2.22
	Mean	1.92	2.68	3.6	5.4

Note: The data show the mean of 100 cells analyzed (\pm standard deviation), for each individual for the low dose range (0–10 cGy).

Table 2. Average values of gamma-H2AX foci per cell for high dose range

		Dose [cGy]				
Donors		50	100	200	300	500
Gamma-H2AX foci/per cell (average of 100 cells per dose point)	Individual 1	8.19 \pm 1.64	9.85 \pm 3.98	12.84 \pm 4.09	16.74 \pm 4.34	19.27 \pm 3.46
	Individual 2	8.48 \pm 1.57	9.96 \pm 2.68	11.31 \pm 3.78	15.09 \pm 3.90	18.98 \pm 2.51
	Individual 3	9.03 \pm 1.40	8.58 \pm 1.76	12.38 \pm 2.23	14.29 \pm 2.72	18.92 \pm 3.40
	Individual 4	6.13 \pm 2.69	7.41 \pm 1.64	12.22 \pm 2.89	14.41 \pm 2.38	18.14 \pm 3.52
	Individual 5	6.18 \pm 2.43	7.78 \pm 2.36	10.5 \pm 2.22	15.05 \pm 2.94	17.65 \pm 3.60
	Mean	7.6	8.72	11.85	15.12	18.59

Note: The data show the mean of 100 cells analyzed (\pm standard deviation), for each individual for the high dose range (50–500 cGy)

Table 3. Estimated dose using the linear mathematical expression derived from the low dose- response curve

Donor	Test dose [cGy]	Gamma-H2AX foci per cell (average of 100 cells)	Linear fit mathematical expression obtained from the low dose-response curve	Estimated dose [cGy]	Dose difference [cGy]
Individual 6	7.5	4.88 \pm 2.45	$x = (y - 2.0916) / 0.3271$	8.52	+ 1.02
Individual 7	7.5	4.84 \pm 2.50		8.40	+ 0.90

Table 4. Estimated dose using the linear mathematical expression derived from the high dose-response curve

Donor	Test dose [cGy]	Gamma-H2AX foci per cell (average of 100 cells)	Linear fit mathematical expression obtained from the high dose-response curve	Estimated dose [cGy]	Dose difference [cGy]
Individual 6	250	12.28 ± 2.71	$x = (y - 6.0456) / 0.0267$	233.50	-16.50
Individual 7	250	12.04 ± 3.08		224.51	-25.49

using the equation 4 and was found to have a dose difference of - 16.50 cGy and - 25.49 cGy as shown in Table 4.

Integrated low and high dose-response curve

An effort to integrate the determined low and high dose-response curve was carried out. It was found that from 0–500 cGy the best fit was computed and found to be linear quadratic in nature (Fig. 6) and the corresponding mathematical expression is as follows:

$$y = -5 \times 10^{-05} x^2 + 0.0547x + 3.4618 \quad (5)$$

$$x = \frac{-\alpha + \sqrt{[\alpha^2 + 4\beta(y - c)]}}{2\beta} \quad (6)$$

where:

- y is the mean gamma-H2AX foci per cell,
- x is the dose (cGy),
- α coefficient is 0.0547,
- β coefficient is -5×10^{-5} ,
- Intercept C = 3.4618,

The corresponding R² value was found to be 0.9706 and equation 6 was used to estimate the de-

livered test dose. Overlapping of gamma-H2AX foci was identified from 10 cGy. Dose estimated using linear-quadratic fit showed more uncertainties when compared to dose estimated by the individualized low and high dose response curves. The dose difference, for the low doses were found to be + 19.07, + 18.30 cGy and - 53.49, - 60.27 cGy for high doses as shown in Table 5.

Imperative steps in the standardization of gamma-H2AX immunofluorescence method

The standardization involved two vital steps to achieve perceivable image quality on gamma-H2AX foci. At first, the gamma-H2AX assay was performed without the use of cytospin, and only a few cells could be observed per microscopic view due to non-adherence of cells (Fig. 7A). After the inclusion of cytospin centrifugation, an evenly distributed monolayer of cells per microscopic view was noted. Two slides (slide A and slide B) were loaded with PMBCs in which the slide A consisted of 10 μL of PBMCs and slide B consisted of 20 μL of PBMCs in a cytofunnel chamber and cytospin centrifuge was performed at 500 rpm

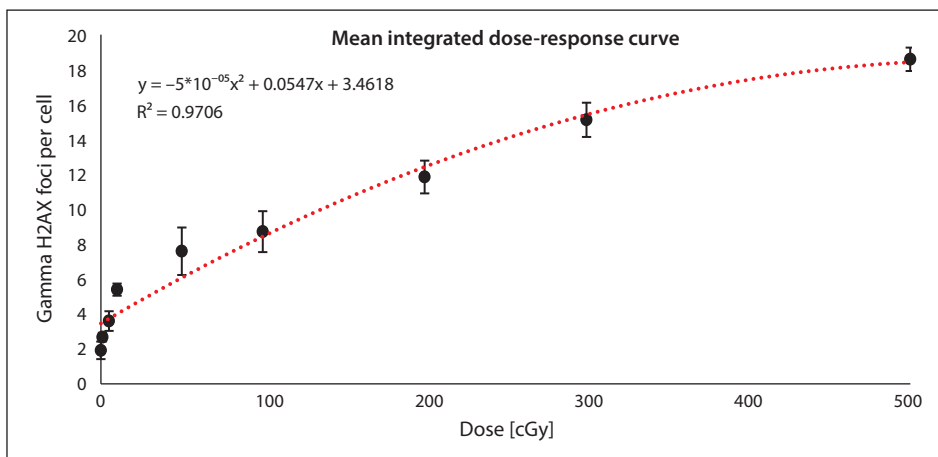
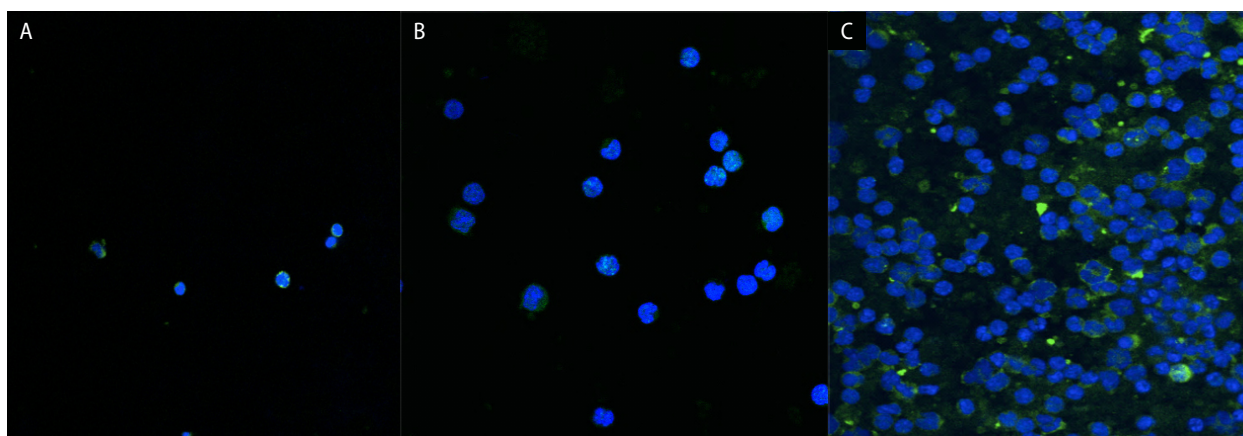
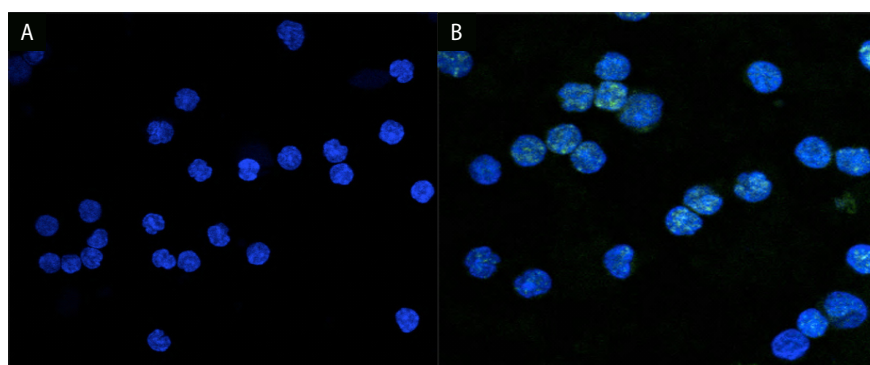


Figure 6. Mean gamma-H2AX foci per cell for integrated dose-response curve of five individuals. [(100 cells per dose point) × 5 individuals = 500 cells in total per dose point] was plotted in this graph]. The error bars represent standard deviation. Linear-quadratic model was fit and the mathematical expression for the same was computed

Table 5. Estimated dose using the linear quadratic mathematical expression derived from the integrated dose-response curve

Donor	Test dose [cGy]	Gamma-H2AX foci cell (average of 100 cells)	Linear quadratic mathematical expression obtained from the integrated dose-response curve	Estimated dose [cGy]	Dose difference [cGy]
Individual 6	7.5	4.88 ± 2.45	$x = \frac{-\alpha + \sqrt{[\alpha^2 + 4\beta(y - c)]}}{2\beta}$	26.57	19.07
	250	12.28 ± 2.71		196.51	-53.49
Individual 7	7.5	4.84 ± 2.50		25.80	18.30
	250	12.04 ± 3.08		189.73	-60.27

**Figure 7.** **A.** Irradiated cells without cytopspin shows the dispersion of cells with lesser number of cell nuclei per microscopic view (cytofunnel chamber loaded with 20 µL of PBMCs); **B.** Evenly deposited monolayer of irradiated cells after cytopspin in slide A [cytofunnel chamber loaded with 10 µL of peripheral blood mononuclear cells (PBMCs)]; **C.** Evenly deposited monolayer with excessive amount of overlap and background of irradiated cells after cytopspin in slide B (cytofunnel chamber loaded with 20 µL of PBMCs)**Figure 8.** **A.** Poor differentiation of gamma-H2AX foci in irradiated cells was observed after 1-hour primary and 1/2-hour secondary antibody incubation; **B.** Optimal differentiation of gamma-H2AX foci was observed in irradiated cells after 2-hour primary and 1-hour secondary antibody incubation

for 5 minutes. It was observed that when 10 µL of PBMCs was loaded the cells could be viewed without overlapping and thereby improving the quality of image analysis (Fig. 7A–C). Further to improve the visualization of gamma-H2AX foci, primary

antibody and secondary antibody incubation time was doubled from 1 hour to 2 hours, and 1/2 hour to 1 hour, respectively. Better differentiation of gamma-H2AX foci was observed in irradiated cells during image analysis as shown in Figure 8.

Table 6. Time and cost required to complete each step involved in gamma-H2AX immunofluorescence assay

S. No	Steps involved	Time for completion of each step	Notes	Items of cost in rupees
1	PBMC isolation	30 minutes	Gradient centrifuge method	100 mL of histopaque — 3000/-
2	PBS wash	5 minutes	3100 rpm for 5 min.	0/-
3	Activation of histone phosphorylation	30 minutes	Activated using FBS	500 mL — 52,170/-
4	PBS wash	5 minutes	3100 rpm for 5 min	0/-
5	Cell fixation	15 minutes	Section: 2.6	1 gram of paraformaldehyde: 14,141/-
6	PBS wash	5 minutes	3100 rpm for 5 min	0/-
7	Antigen retrieval and protein blocking	30 minutes	Section: 2.6	10,367/-
8	PBS wash	5 minutes	3100 rpm for 5 min	0/-
9	Primary antibody incubation	120 minutes	Section: 2.6	20 microlitre — 13,189/-
10	PBS wash	5 minutes	3100 rpm for 5 min	0/-
11	Secondary antibody incubation	60 minutes	Section: 2.6	1 mg — 26,135/-
12	Nuclear Staining using DAPI	5 minutes	Section: 2.6	10 mg — 3000/-
13	Cytospin	10 minutes	5 minutes for loading cells in cytofunnel chamber + 5 minutes for cytospin at 500 rpm	300/- per sample
14	Microscopy	30 minutes	Gamma-H2AX foci captured using confocal laser scanning microscope	1000/- per hour
15	Image analysis	60 minutes	Software used: Fiji	Open source freely available on online
	Total time and cost for establishment of lab	7 hours and 30 minutes		1,20,602/-

PBMC — peripheral blood mononuclear cells; PBS — phosphate-buffered saline; FBS — fetal bovine serum. DAPI — 4',6-diamidino-2-phenylindole

Time and cost requirement for gamma-H2AX immunofluorescence assay

The time required and the expenses incurred to complete gamma-H2AX assay is tabulated as shown in Table 6. It was observed that total time required to complete the assay is 7 hours and 30 minutes. A total cost of 1,20,602 rupees (~1468 USD) was expended to establish the gamma-H2AX immunofluorescence method. The confocal laser scanning microscope and the cytospin was already available in our institution and the expended cost was calculated based on usage per hour. An approximate amount of 5000 rupees (~60 USD) per sample would be required for immunofluorescence-based gamma-H2AX analysis which includes the man power and microscopy usage.

Discussion

As gamma-H2AX biomarker has been found to be an effective indicator for tracking DNA DSBs [21], we have investigated the potential use of gamma-H2AX assay as a biological dosimeter by determining the dose-response curve for low and high doses followed by test dose verification. Additionally, an integrated dose-response curve, combining the low and high dose-response curves was also determined.

In our work, the time frame of processing samples and to eliminate the influence of repair which would have led to reduction in foci numbers, a time interval of 2 hours between the time of irradiation to sample processing was maintained constant throughout the entire research work [7]. The gamma-H2AX foci per cell in the PBMC control cells

(0 Gy) were found to be 1.92 ± 0.49 , on average, obtained from five individuals. Our results were comparable to the data published by Parris et al., where they measured 2.13 foci per cell in control cells in MRC5-SV1 cells without using extended depth of focus [22]. The measurement of DNA damage in control cells plays a significant role during the initial standardization process as it represents the satisfactory preparation condition for analysis of gamma-H2AX foci per cell.

The dose-response curves (dose vs gamma-H2AX foci) determined for low and high dose radiation had a good correlation with dose, where the goodness of fit R^2 values were found to be 0.9829 and 0.9766, respectively. This proves that with an increase in radiation dose, higher number of DNA DSBs and, thereby, a proportional increase in the number of gamma-H2AX foci can be observed [7, 23]. Grudzenski et al. performed gamma-H2AX assay in human fibroblasts for low doses and found that elevated levels of gamma-H2AX were identified with increase in low levels of radiation [24]. Moquet et al. exposed the human lymphocytes to high doses 0.2 to 4.3 Gy and found that gamma-H2AX assay had a strong correlation with high doses of radiation [9]. Based on our data, it was found that this assay could be suitable to estimate doses and evaluate the DNA DSBs in both low and high dose ranges.

From our observation, it was noted that at doses higher than 10 cGy, gamma-H2AX foci density increased due to the overlapping effect with the nearby foci. This overlapping effect could be clearly understood from the integrated dose response curve (Fig. 6) where one could observe that gamma-H2AX foci per cell follows a linear trend from 0 to 10 cGy beyond which the curve bends downward between 10 and 50 cGy and resumes the linear trend in the range 50 to 500 cGy. The overlapping of the gamma-H2AX foci at doses of 1 Gy induced by alpha radiation was observed by Abu Shqair et al. [25].

For the test doses, the doses estimated using individual calibration curves were accurate as compared to the doses estimated using the integrated linear quadratic dose-response curve. This emphasizes the need to have individual dose-response calibration curves for both low and high doses of ionizing radiation. From our study the time re-

quired to estimate dose with the gamma-H2AX assay was found to be 7 hours and 30 minutes while the time required using the “gold standard” DCA was about 3–4 days as reported in literature [5, 6]. Hence, we find that the gamma-H2AX immunofluorescence method could be used as a rapid biodosimetric tool. This study validates the use of gamma H2AX for acute exposure and this calibration model cannot be used for chronic exposures as the effect of repair would affect the foci counts. Further considerations on the determination of the dose-response curves for different time points beyond the two-hour time period maintained in this study, have to be experimentally studied and analysed as gamma H2AX experiences fading due to dephosphorylation (10). Redon et al. used the gamma H2X assay to determine dose response curves using animal models (rhesus macaque (*Macaca mulatta*) model) [26]. Further validation of our calibration data with animal models could be an intermediate step prior to clinical use.

Conclusion

In this research work, we have determined and validated the dose-response calibration curves using gamma-H2AX immunofluorescence assay. Based on our findings, we infer that the individual dose-response calibration curves for both low and high dose ranges of gamma radiation can be used for biological dosimetry. Further, the short time required to complete the gamma-H2AX immunofluorescence assay proves that it can be used as a rapid biodosimetric tool for cost-effective dose estimation in institutions with an existing confocal microscope facility.

Acknowledgements

This research is a part of the Ph.D. thesis work of the first author who is registered under The Tamil Nadu Dr. M.G.R. Medical University, Chennai, India. Authors would like to thank the Centre for Stem Cell Research Imaging Core facility (A unit of inStem, Bengaluru), Christian Medical College Campus, Bagayam, India for providing the imaging slots.

Conflicts of interest

The authors declare none.

Funding

This research work was funded by internal fluid research [IRB No 11242] grant of Christian Medical College Vellore.

Ethical standards

The study was carried out in accordance with the ethical standards of the responsible committee and has been approved by institutional ethics committee — Christian Medical College Vellore.

References

1. Sorokine-Durm I, Durand V, Le Roy A, et al. Is FISH painting an appropriate biological marker for dose estimates of suspected accidental radiation overexposure? A review of cases investigated in France from 1995 to 1996. *Environ Health Perspect.* 1997; 105 Suppl 6(Suppl 6): 1427–1432, doi: [10.1289/ehp.97105s61427](https://doi.org/10.1289/ehp.97105s61427), indexed in Pubmed: [9467056](https://pubmed.ncbi.nlm.nih.gov/9467056/).
2. International Atomic Energy Agency. *Cytogenetic Dosimetry: Applications in Preparedness for and Response to Radiation Emergencies, Emergency Preparedness and Response*. IAEA, Vienna 2011: 247.
3. Macià I Garau M, Lucas Calduch A, López EC. Radiobiology of the acute radiation syndrome. *Rep Pract Oncol Radiother.* 2011; 16(4): 123–130, doi: [10.1016/j.rpor.2011.06.001](https://doi.org/10.1016/j.rpor.2011.06.001), indexed in Pubmed: [24376969](https://pubmed.ncbi.nlm.nih.gov/24376969/).
4. Boice JD. The linear nonthreshold (LNT) model as used in radiation protection: an NCRP update. *Int J Radiat Biol.* 2017; 93(10): 1079–1092, doi: [10.1080/09553002.2017.1328750](https://doi.org/10.1080/09553002.2017.1328750), indexed in Pubmed: [28532210](https://pubmed.ncbi.nlm.nih.gov/28532210/).
5. Gnanasekaran TS. Cytogenetic biological dosimetry assays: recent developments and updates. *Radiat Oncol J.* 2021; 39(3): 159–166, doi: [10.3857/roj.2021.00339](https://doi.org/10.3857/roj.2021.00339), indexed in Pubmed: [34610654](https://pubmed.ncbi.nlm.nih.gov/34610654/).
6. Ryan TL, Pantelias AG, Terzoudi GI, et al. Use of human lymphocyte G0 PCCs to detect intra- and inter-chromosomal aberrations for early radiation biodosimetry and retrospective assessment of radiation-induced effects. *PLoS One.* 2019; 14(5): e0216081, doi: [10.1371/journal.pone.0216081](https://doi.org/10.1371/journal.pone.0216081), indexed in Pubmed: [31059552](https://pubmed.ncbi.nlm.nih.gov/31059552/).
7. Eberlein U, Peper M, Fernández M, et al. Calibration of the γ -H2AX DNA double strand break focus assay for internal radiation exposure of blood lymphocytes. *PLoS One.* 2015; 10(4): e0123174, doi: [10.1371/journal.pone.0123174](https://doi.org/10.1371/journal.pone.0123174), indexed in Pubmed: [25853575](https://pubmed.ncbi.nlm.nih.gov/25853575/).
8. Turner HC, Brenner DJ, Chen Y, et al. Adapting the γ -H2AX assay for automated processing in human lymphocytes. 1. Technological aspects. *Radiat Res.* 2011; 175(3): 282–290, doi: [10.1667/RR2125.1](https://doi.org/10.1667/RR2125.1), indexed in Pubmed: [21388271](https://pubmed.ncbi.nlm.nih.gov/21388271/).
9. Moquet J, Barnard S, Rothkamm K. Gamma-H2AX biodosimetry for use in large scale radiation incidents: comparison of a rapid '96 well lyse/fix' protocol with a routine method. *PeerJ.* 2014; 2: e282, doi: [10.7717/peerj.282](https://doi.org/10.7717/peerj.282), indexed in Pubmed: [24688860](https://pubmed.ncbi.nlm.nih.gov/24688860/).
10. Wanotayan R, Wongsanit S, Boonsirichai K, et al. Quantification of histone H2AX phosphorylation in white blood cells induced by ex vivo gamma irradiation of whole blood by both flow cytometry and foci counting as a dose estimation in rapid triage. *PLoS One.* 2022; 17(3): e0265643, doi: [10.1371/journal.pone.0265643](https://doi.org/10.1371/journal.pone.0265643), indexed in Pubmed: [35320288](https://pubmed.ncbi.nlm.nih.gov/35320288/).
11. Chang DS, Lasley FD, Das IJ, Mendonca MS, Dynlacht JR. *Basic Radiotherapy Physics and Biology* [Internet]. Cham: Springer International Publishing; 2021. <http://link.springer.com/10.1007/978-3-030-61899-5> (18.01.2023).
12. Vignard J, Mirey G, Salles B. Ionizing-radiation induced DNA double-strand breaks: a direct and indirect lighting up. *Radiother Oncol.* 2013; 108(3): 362–369, doi: [10.1016/j.radonc.2013.06.013](https://doi.org/10.1016/j.radonc.2013.06.013), indexed in Pubmed: [23849169](https://pubmed.ncbi.nlm.nih.gov/23849169/).
13. Arya G, Schlick T. A tale of tails: how histone tails mediate chromatin compaction in different salt and linker histone environments. *J Phys Chem A.* 2009; 113(16): 4045–4059, doi: [10.1021/jp810375d](https://doi.org/10.1021/jp810375d), indexed in Pubmed: [19298048](https://pubmed.ncbi.nlm.nih.gov/19298048/).
14. Foster ER, Downs JA. Histone H2A phosphorylation in DNA double-strand break repair. *FEBS J.* 2005; 272(13): 3231–3240, doi: [10.1111/j.1742-4658.2005.04741.x](https://doi.org/10.1111/j.1742-4658.2005.04741.x), indexed in Pubmed: [15978030](https://pubmed.ncbi.nlm.nih.gov/15978030/).
15. Johansson P, Muslimovic A, Hultborn R, et al. In-solution staining and arraying method for the immunofluorescence detection of γ H2AX foci optimized for clinical applications. *Biotechniques.* 2011; 51(3): 185–189, doi: [10.2144/000113738](https://doi.org/10.2144/000113738), indexed in Pubmed: [21906040](https://pubmed.ncbi.nlm.nih.gov/21906040/).
16. Kuo LJ, Yang LX. Gamma-H2AX - a novel biomarker for DNA double-strand breaks. *In Vivo.* 2008; 22(3): 305–309, indexed in Pubmed: [18610740](https://pubmed.ncbi.nlm.nih.gov/18610740/).
17. Redon CE, Nakamura AJ, Sordet O, et al. γ -H2AX detection in peripheral blood lymphocytes, splenocytes, bone marrow, xenografts, and skin. *Methods Mol Biol.* 2011; 682: 249–270, doi: [10.1007/978-1-60327-409-8_18](https://doi.org/10.1007/978-1-60327-409-8_18), indexed in Pubmed: [21057933](https://pubmed.ncbi.nlm.nih.gov/21057933/).
18. Chaurasia RK, Bhat NN, Gaur N, et al. Establishment and multiparametric-cytogenetic validation of Co-gamma-ray induced, phospho-gamma-H2AX calibration curve for rapid biodosimetry and triage management during radiological emergencies. *Mutat Res Genet Toxicol Environ Mutagen.* 2021; 866: 503354, doi: [10.1016/j.mrgentox.2021.503354](https://doi.org/10.1016/j.mrgentox.2021.503354), indexed in Pubmed: [33985694](https://pubmed.ncbi.nlm.nih.gov/33985694/).
19. Ricoul M, Gnana Sekaran TS, Brochard P, et al. γ -H2AX Foci Persistence at Chromosome Break Suggests Slow and Faithful Repair Phases Restoring Chromosome Integrity. *Cancers (Basel).* 2019; 11(9), doi: [10.3390/cancers11091397](https://doi.org/10.3390/cancers11091397), indexed in Pubmed: [31546867](https://pubmed.ncbi.nlm.nih.gov/31546867/).
20. Schindelin J, Arganda-Carreras I, Frise E, et al. Fiji: an open-source platform for biological-image analysis. *Nat Methods.* 2012; 9(7): 676–682, doi: [10.1038/nmeth.2019](https://doi.org/10.1038/nmeth.2019), indexed in Pubmed: [22743772](https://pubmed.ncbi.nlm.nih.gov/22743772/).
21. Visweswaran S, Joseph S, Dhanasekaran J, et al. Exposure of patients to low doses of X-radiation during neuro-interventional imaging and procedures: Dose estimation and analysis of γ -H2AX foci and gene expression in blood lymphocytes. *Mutat Res Genet Toxicol Environ Mutagen.* 2020; 856-857: 503237, doi: [10.1016/j.mrgentox.2020.503237](https://doi.org/10.1016/j.mrgentox.2020.503237), indexed in Pubmed: [32928370](https://pubmed.ncbi.nlm.nih.gov/32928370/).
22. Parris CN, Adam Zahir S, Al-Ali H, et al. Enhanced γ -H2AX DNA damage foci detection using multimagnification and extended depth of field in imaging flow cytometry. *Cytometry A.* 2015; 87(8): 717–723, doi: [10.1002/cyto.a.22697](https://doi.org/10.1002/cyto.a.22697), indexed in Pubmed: [26087127](https://pubmed.ncbi.nlm.nih.gov/26087127/).
23. Moquet J, Barnard S, Staynova A, et al. The second gamma-H2AX assay inter-comparison exercise carried

- out in the framework of the European biodosimetry network (RENEB). *Int J Radiat Biol.* 2017; 93(1): 58–64, doi: [10.1080/09553002.2016.1207822](https://doi.org/10.1080/09553002.2016.1207822), indexed in Pubmed: [27686523](https://pubmed.ncbi.nlm.nih.gov/27686523/).
24. Grudzenski S, Raths A, Conrad S, et al. Inducible response required for repair of low-dose radiation damage in human fibroblasts. *Proc Natl Acad Sci U S A.* 2010; 107(32): 14205–14210, doi: [10.1073/pnas.1002213107](https://doi.org/10.1073/pnas.1002213107), indexed in Pubmed: [20660770](https://pubmed.ncbi.nlm.nih.gov/20660770/).
25. Abu Shqair A, Lee US, Kim EH. Computational modelling of γ -H2AX foci formation in human cells induced by alpha particle exposure. *Sci Rep.* 2022; 12(1): 14360, doi: [10.1038/s41598-022-17830-8](https://doi.org/10.1038/s41598-022-17830-8), indexed in Pubmed: [35999233](https://pubmed.ncbi.nlm.nih.gov/35999233/).
26. Redon CE, Nakamura AJ, Gouliava K, et al. The use of gamma-H2AX as a biodosimeter for total-body radiation exposure in non-human primates. *PLoS One.* 2010; 5(11): e15544, doi: [10.1371/journal.pone.0015544](https://doi.org/10.1371/journal.pone.0015544), indexed in Pubmed: [21124906](https://pubmed.ncbi.nlm.nih.gov/21124906/).